Fungal Genetics and Biology 82 (2015) 213–227

Contents lists available at ScienceDirect

Fungal Genetics and Biology

journal homepage: www.elsevier.com/locate/yfgbi

Two microtubule-plus-end binding proteins LIS1-1 and LIS1-2, homologues of human LIS1 in *Neurospora crassa*

Olga A. Callejas-Negrete [a], Michael Plamann [b], Robert Schnittker [b], Salomon Bartnicki-García [a], Robert W. Roberson [c], Genaro Pimienta [a], Rosa R. Mouriño-Pérez [a,*]

[a] Departamento de Microbiología, Centro de Investigación Científica y de Educación Superior de Ensenada (CICESE), Ensenada, B.C., Mexico
[b] School of Biological Sciences, University of Missouri-Kansas City, Kansas City, MO, USA
[c] School of Life Sciences, Arizona State University, Tempe, AZ, USA

ARTICLE INFO

Article history:
Received 8 April 2015
Revised 26 July 2015
Accepted 27 July 2015
Available online 29 July 2015

Keywords:
LIS1
Microtubules
Dynein–dynactin
Neurospora crassa
+TIP proteins

ABSTRACT

LIS1 is a microtubule (Mt) plus-end binding protein that interacts with the dynein/dynactin complex. In humans, LIS1 is required for proper nuclear and organelle migration during cell growth. Although gene duplication is absent from *Neurospora crassa*, we found two paralogues of human LIS1. We named them LIS1-1 and LIS1-2 and studied their dynamics and function by fluorescent tagging. At the protein level, LIS1-1 and LIS1-2 were very similar. Although, the characteristic coiled-coil motif was not present in LIS1-2. LIS1-1-GFP and LIS1-2-GFP showed the same cellular distribution and dynamics, but LIS1-2-GFP was less abundant. Both LIS1 proteins were found in the subapical region as single fluorescent particles traveling toward the cell apex, they accumulated in the apical dome forming prominent short filament-like structures, some of which traversed the Spitzenkörper (Spk). The fluorescent structures moved exclusively in anterograde fashion along straight paths suggesting they traveled on Mts. There was no effect in the filament behavior of LIS1-1-GFP in the Δ*lis1-2* mutant but the dynamics of LIS1-2-GFP was affected in the Δ*lis1-1* mutant. Microtubular integrity and the dynein–dynactin complex were necessary for the formation of filament-like structures of LIS1-1-GFP in the subapical and apical regions; however, conventional kinesin (KIN-1) was not. Deletion mutants showed that the lack of *lis1-1* decreased cell growth by ~75%; however, the lack of *lis1-2* had no effect on growth. A Δ*lis1-1*;Δ*lis1-2* double mutant showed slower growth than either single mutant. Conidia production was reduced but branching rate increased in Δ*lis1-1* and the Δ*lis1-1*;Δ*lis1-2* double mutants. The absence of LIS1-1 had a strong effect on Mt organization and dynamics and indirectly affected nuclear and mitochondrial distribution. The absence of LIS1-1 filaments in dynein mutants (ropy mutants) or in benomyl treated hyphae indicates the strong association between this protein and the regulation of the dynein–dynactin complex and Mt organization. LIS1-1 and LIS1-2 had a high amino acid homology, nevertheless, the absence of the coiled-coil motif in LIS1-2 suggests that its function or regulation may be distinct from that of LIS1-1.

1. Introduction

As in all eukaryotes, the fungal cytoskeleton is a dynamic structure that maintains shape, organization and support of cytoplasmic components, control of cell movements, and plays important roles in both vesicles and organelles intracellular transport and cellular division. Mts are 25 nm diameter tubular assemblies of a heterodimeric protein made of α-β tubulin subunits, with a combined molecular weight of ~110 kDa (Garvalov et al., 2006). The dimers are aligned head-to-tail to form ~13 linear polymers called protofilaments that run lengthwise along Mts and associate laterally to form the closed Mts wall (Oakley and Morris, 1980; Derksen and Emons, 1990; Haimo, 1997; Nédélec et al., 2003). This arrangement confers on Mts a structural polarity, they have a plus and a minus end. The Mt plus end is the more dynamic, it polymerizes and depolymerizes rapidly (Oakley, 2000). Most Mts are parallel to the longitudinal axis of the cells, but perpendicular to the mitochondria, multivesicular bodies, nuclei and secretory vesicles (Howard and Aist, 1980; Derksen and Emons, 1990; Haimo, 1997; Mouriño-Pérez et al., 2006).

Mechanical forces generated by Mt-based motor proteins are thought to play an important role in Mt dynamics. The motor

* Corresponding author at: P.O. Box 430222, San Ysidro, CA, USA.
E-mail address: rmourino@cicese.mx (R.R. Mouriño-Pérez).

http://dx.doi.org/10.1016/j.fgb.2015.07.009
1087-1845/

proteins dynein/dynactin complex and other motor proteins of the kinesin family are present in all eukaryotes. Motor proteins use the energy of ATP hydrolysis to move along Mts in a unidirectional manner, transporting organelles or sliding Mts toward either the MT plus or minus end (Hirokawa, 1998). The proposed functions of motors include Mt dynamics control during cell growth and division (Xiang and Plamann, 2003). The dynein/dynactin complex is a multi-subunit motor protein that is minus end-directed. In filamentous fungi, dynein is used for retrograde transport of vesicles and organelles (Seiler et al., 1999). Dynein mutants have shown defects in organelle organization and transport and in the Spk stability (Xiang and Plamann, 2003).

LIS1 is a human Mt associated protein that has been implicated in the regulation of the dynein/dynactin complex, a major Mt motor protein (Vallee and Tsai, 2006). Sporadic mutations in the human *lis1* gene produce lissencephaly or 'smooth brain', a severe brain disease characterized by mislocalization of cortical neurons (Reiner et al., 1995; Izumi et al., 2007). The symptoms are mental deficiency, epilepsy and a smooth brain surface (Miller, 1963; Dieker et al., 1969; Barth et al., 1982; Dobyns, 1989; Dobyns et al., 1991). LIS1 seems to be involved in the process of neuron migration. Normally, neurons migrate from the paraventricular proliferative region and populate the cerebral cortex turning it convoluted. In patients with lissencephaly, neuron migration is retarded and consequently there is an underpopulation of neurons in the cortex preventing it from becoming convoluted. Biochemical studies have shown that the possible function(s) of LIS1 are related to its association with Mts. LIS1 has been reported to co-purify with platelet-activating-factor acetyl hydrolase (Hattori et al., 1994), which increases the frequency of a microtubular catastrophe event *in vitro* (Sapir et al., 1997).

In *Aspergillus nidulans*, *nudF* is the homologue of the *lis1* gene (Xiang et al., 1995; Morris et al., 1998). It was identified as part of a group of proteins involved in nuclear migration, such as NudC (Osmani et al., 1990), ApsA and ApsB (Morris et al., 1995). In *A. nidulans*, NudF appears to be crucial for nuclear migration during vegetative growth and reproduction, both sexual and asexual. NudF can be found moving linearly on Mts along the hyphae and accumulating as filaments at the Mt plus ends (Han et al., 2001; Zhang et al., 2003; Efimov, 2003).

In *Neurospora crassa*, there is not one but two homologues of LIS1 protein, LIS1-1 and LIS1-2. This duality poses intriguing questions about its significance. Accordingly, the goal of this study was to describe the localization and cellular dynamics of LIS1-1 and LIS1-2 using live-cell imaging methods and to analyze the phenotypes of single and double deletion mutants of these two genes. We also examined the relationship of LIS1-1 and LIS1-2 to the main Mt motor proteins, the dynein–dynactin complex and conventional kinesin. Additionally, we discussed the significance of having two paralogues of LIS1 in the genome of *N. crassa*.

2. Materials and methods

2.1. Strains and culture conditions

Strains used in this study are listed in Table 1. Strains were maintained on Vogel's minimal medium (VMM) with 2% sucrose. All manipulations were according to standard techniques (Davis, 2000).

2.2. Construction of plasmids containing lis1-1 and lis1-2 gene fusions expressing fluorescent tagged proteins

Standard PCR and cloning procedures (Sambrook et al., 1989) were used to fuse the *sgfp* gene to the end of the *lis1-1* and *lis1-2* structural genes. The *lis1-1* and *lis1-2* genes were amplified by PCR from *N. crassa* (FGSC 2489) genomic DNA. Primers used are listed in Table 1. PCR was performed in an Apollo Thermal Cycler with Platinum Hi-fi Taq polymerase (Invitrogen, Carlsbad, CA) according to the manufacturer's instructions. Amplified and gel-purified PCR products were digested with XbaI and PacI and ligated into XbaI- and PacI-digested plasmid pMF272 (GenBank accession No. AY598428) for GFP tagging and pJV15-2 for mChFP (Verdín et al., 2009). The resulting expression plasmids were pRM04-OC03, pRM13-OC06, pRM23-OC16 and pRM22-OC15 containing the gene fusions *lis1-1-sgfp*, *lis1-2-sgfp*, *lis1-1-mChPF* and *lis1-2-mChPF*, respectively (Table 1). All plasmids were verified by sequencing at Eton Biosciences (San Diego, CA).

2.3. Construction of lis1-1 fusion constructs under native promoter

We also fused *lis1-1* at the 3′ end of the open reading fame (ORF) by a split marker "knock-in" procedure. Construction of the recombinant dsDNA for the "knock-in" technique was achieved by split marker fusion PCR. Six primers were designed to generate the cassettes used in transformations (Table 1). For each sequence, primers number one (P1) are forward primers to amplify ~1000 bp (3′) of each *lis1* ORF; P2 are designed as ~30–40 bp reverse primers to the 3′ regions of the *lis1* ORF (15–20 bp) excluding stop codons and the 5′ regions of the tags (15–20 bp); P3 are ~30–40 bp forward primers to the 5′ regions of the 3′ untranslated regions (UTR) of the *lis1* genes and the 3′ regions of the tags; P4 are reverse primers to amplify ~1000 bp (5′) of the 3′ UTR of the *lis1* genes. P5 are forward primers to the selective marker and P6 are reverse primers to the selective marker. P1 and P2 as well as P3 and P4 were used for the first round of PCR using genomic DNA as template. Those reactions lead to PCR amplicon 1 (PCRp1) and PCR amplicon 2 (PCRp2) respectively. The two PCR amplicons (PCRp1 and PCRp2) were purified and used as templates for the second round of PCR, where PCRp1 and PCRp2 and the tag-selective marker sequences were used as templates. The primers used for the second PCR round were P1, P4, P5 and P6, where P5 are forward primers to the hygromycin resistance cassette (*hph*) sequence and P6 are reverse primers to *hph* sequence.

2.4. Transformation protocols, transformant selection and crosses

Transformation of *N. crassa* (FGSC9717 Δ*mus-51*; *his-3*$^{-}$) conidia with non-linearized plasmids (Table 1) was carried out by electroporation on a Bio-Rad Gene Pulser (capacitance, 25 μF; 1.5 kV; resistance, 600 Ω) as previously described (Margolin et al., 1997). Prototrophic His^{+} transformants were screened for the expression of GFP or mChFP by epifluorescence microscopy as described previously (Freitag et al., 2004). Initial transformants showing strong fluorescence were often heterokaryons. To obtain pure strains containing integrated DNA, transformants were crossed to strain NMF161, and progeny were isolated (Davis, 2000).

To generate strains containing knock-in constructs, the two fragments were obtained (gene-tag-partial marker, partial marker-3′ UTR) and used to transform a *N. crassa* Δ*mus-51* strain (FGSC #9718) selecting for hygromycin resistance (Ninomiya et al., 2004). (Note: the Δ*mus-51* marker reduces the frequency of non-homologous integration of transforming sequences resulting in 95–100% homologous recombination.) In the resulting transformants, the recombinant dsDNA tagged *lis1* sequences replaced the endogenous copy of *lis1-1*.

In order to express the tagged *lis1* genes of interest in the Δ*lis1-1* and Δ*lis1-2* backgrounds, we produced double mutants Δ*lis1-1*;*his-3*$^{-}$ and Δ*lis1-2*;*his-3*$^{-}$ to target the vectors to the *his-3* locus by crossing the respective *lis1* mutants with a *his-3*$^{-}$ strain. We selected progeny from these crosses that grew in media

Table 1
Materials used. *N. crassa* strains, plasmids and oligonucleotides.

Name	Genotype, description, or sequence	Reference
Strains		
FGSC2225	*mat A Wildtype*	FGSC
FGSC4200	*mat a Wildtype*	FGSC
FGSC9717	*mat A-Δmus*$^{-51}$*-his-3*$^{-}$	FGSC
TRM004-OC03	*mat A lis1-1-sgfp-his-3*$^{+}$	This study
TRM013-OC06	*mat A lis1-2-sgfp- his-3*$^{+}$	This study
TRM106-OC41	*mat A Pccg-1- β -tub-mCherry*$^{+}$*; his-3*$^{+}$*::LIS1-1-sgfp*	This study
TRM107-OC42	*mat A Δro-3; his-3*$^{+}$*::Pccg-1-lis1-1-sgfp*$^{+}$	This study
TRM108-OC43	*mat A Δro-1; his-3*$^{+}$*::Pccg-1-lis1-1-sgfp*$^{+}$	This study
TRM109-OC44	*mat A Δkin-1; his-3*$^{+}$*::Pccg-1-lis1-1-sgfp*$^{+}$	This study
TRM110-OC45	*mat A Δlis1-1;his-3*$^{-}$	This study
TRM111-OC46	*mat A Δlis1-2; his-3*$^{-}$	This study
TRM112-OC47	*mat A Δlis1-1;mat A his-3*$^{+}$*::Pccg-1- β-tub-sgfp*$^{+}$	This study
TRM113-OC48	*mat A Δlis1-2; mat A his-3*$^{+}$*::Pccg-1- β-tub-sgfp*$^{+}$	This study
TRM114-OC49	*mat A Δlis1-1;mat A his-3*$^{+}$*::Pccg-1-lis1-2 -sgfp*$^{+}$	This study
TRM115-OC50	*mat A Δlis1-2; mat A his-3*$^{+}$*::Pccg-1-lis1-1-sgfp*$^{+}$	This study
TMP01	*mat A Δlis1-1*	This study
TMP02	*mat A Δlis1-2*	This study
TMP03	*mat A Δlis1-1;Δlis1-2*	This study
Plasmids		
pMF272	*Pccg-1-sgfp*$^{+}$	Freitag et al. (2004)
pJV-15-2	*Pccg-1-mchfp*$^{+}$	Verdín et al. (2009)
pRM-02-OC01	*Pccg-1-dlic-sgfp*$^{+}$	This study
pRM-04-OC03	*Pccg-1-lis1-1-sgfp*$^{+}$	This study
pRM-06-OC05	*Pccg-1-ro3-sgfp*$^{+}$	This study
pRM-13-OC06	*Pccg-1-lis1-2-sgfp*$^{+}$	This study
pRM-26-ES01	*Pccg-1- β-tub-mchfp*$^{+}$	This study
pRM-71-OC38	*Pccg-1-dlic-mchfp*$^{+}$	This study
pRM-72-OC39	*Pccg-1-ro3-mchfp*$^{+}$	This study
Oligonucleotides		
NUDF-XBAI F	5′ *TACA**TCTAGA**ATGTCCCAAATATTG* 3′	
NUDF-PACI R	5′ *TTTA**TTAATTAA**GTTGGCAAAGATTCTG* 3′	
PAC-1B-XBAI F	5′ *C**TCTAGA**ATGGCTCAAGCTTCAGTT* 3′	
PAC-1B-PACI R	5′ *CC**TTAATTAA**GTTAGCAAAGATCCTAACCT* 3′	
βTUB-SPEI F	5′ *GG**ACTAGT**ATGCGTGAAATTGTAAGTCTC* 3′	
β-TUB-XBAI R	5′ *GC**TCTAGA**CTCCGCCCTCAAGGGGGGCC* 3′	
DLIC-XBAI F	5′ *TATA**TCTAGA**ATGGCGGCCAACACGAAC* 3′	
DLIC-PACI R	5′ *GCAC**TTAATTAA**TGACTGCCGGCTCC* 3′	

containing hygromycin (0.3 mg ml^{-1}), but were unable to grow in media lacking histidine. The double mutants Δ*lis1-1*;*his-3*$^{-}$ and Δ*lis1-2*;*his-3*$^{-}$ were transformed following the procedure described before to label β-tubulin-GFP (pMF309), LIS1-1-GFP (pRM04-OC03), and LIS1-2 -GFP (pRM-13-OC16). We also used the double mutants Δ*lis1-1*;*his-3*$^{-}$ and Δ*lis1-2*;*his-3*$^{-}$ to corroborate the functionality of the *lis1* fusion constructs contained in cassettes pRM04-OC03 and PRM13-OC06. After transformation, the mutants showed wild type (WT) growth suggesting that the tagged *lis1* proteins retained function.

2.5. Co-expression experiments of LIS1-1-GFP and Mt motor proteins tagged with mChFP

To examine the relationship between LIS1-1 and the dynein/dynactin complex and conventional kinesin (KIN-1), we constructed heterokaryons from two strains of *N. crassa*, by vegetatively fusing the *lis1-1*-mChFP strain with strains expressing P150^{GLUED}-GFP, DLIC-*GFP* (dynein light intermediate chain) and/or Kin-1-GFP. For each pair of strains, a VMM plate was inoculated with spores of both strains, and incubated for 10 h at 28 °C. The colonies were screened for hyphae having both fluorescent makers and then carefully imaged following the procedure described below for laser scanning confocal microscopy.

2.6. Measurement of growth kinetics, branching and conidiation rates

To characterize phenotypically Δ*lis1-1*, Δ*lis1-2*, and Δ*lis1-1*;Δ*lis1-2* double mutants, we measure the colony growth rate, hyphal growth rate, biomass production, branching rate, and conidiation rate and also described the colonial and hyphal morphology. The respective knockout strains were constructed by obtaining the deletion cassettes from the *Neurospora* Genome Project and using the methods as described (Colot et al., 2006).

Conidia from each of the *lis1* mutant strains (Δ*lis1-1* and Δ*lis1-2* single mutants and the Δ*lis1-1*;Δ*lis1-2* double mutant) and WT were inoculated in 15 cm-VMM plates (1.5×10^5 spores ml^{-1}) and incubated at 28 °C for 48 h. We calculated the colony growth rate (cm d^{-1}), measuring the colony radius every 6 h in ten different transects. Cultures were done by triplicate. Hyphal elongation rates were measured in time-lapse movies recorded by phase contrast with an inverted microscope Axiovert200® (Carl Zeiss) with an oil immersion objective: 100 × (PH3)/1.3 N.A. Images were captured with 4 s intervals during 5 min and analyzed with the Axiovision® Rel. 4.6.3 software (Carl Zeiss). The rate was calculated with the elongation difference frame by frame, and data was stored and processed in Excel®.

For biomass production, conidia were inoculated (1.5×10^5 - spores ml^{-1}) onto a dialysis membrane covering VMM plates and the plates were incubated at 28 °C for 24 h. The dialysis membranes with mycelium on top were dried out and weighed with an analytical balance (Sartorius model 1712 MP8 Silver Edition). The biomass production was calculated as the weight difference between the dialysis membranes before inoculation and after incubation an expressed in mg d^{-1}.

Strains were inoculated on VMM plates and incubated at 28 °C for 24 h, then observed on an Olympus SZXILLB2-100 (Olympus, Tokyo, Japan) stereomicroscope at a magnification of

400×. Images were captured with an Olympus DP70 CCD camera and analyzed with the accompanying software. The number of lateral branches of 30 leading hyphae was counted in the first 500 μm from the tip (branches/500 μm).

To measure conidia production, VMM plates were inoculated with WT and the different mutant strains and incubated at 28 °C for 6 d. Conidia were collected in five ml of a 1 M sorbitol solution and the conidia were counted using a Neubauer chamber with an Olympus microscope.

2.7. Membrane and organelle fluorescent staining

Using the "inverted agar block method" of preparing and staining samples (Hickey et al., 2002), GFP-expressing strains were incubated with 5 μM FM4-64 (Molecular Probes, Eugene, OR), which labels the plasma membrane and organelle membranes (Fischer-Parton et al., 2000). SytoRed® was used to label mitochondria.

2.8. Laser scanning confocal microscopy

Time-lapse imaging was performed at scan intervals of 0.5–4.5 s for periods up to 40 min. Image resolution was 512 × 512 pixels and 300 dpi. Confocal images were captured using LSM-510 software (version 3.2; Carl Zeiss) and evaluated with an LSM 510 Image Examiner. Some of the image series were converted into AVI movies using the same software. Time-lapse images of hyphae were recorded simultaneously by phase contrast microscopy and fluorescent confocal microscopy. Phase contrast images were captured with a photomultiplier for transmitted light using the same laser illumination for fluorescence (Mouriño-Pérez et al., 2006). Final images were processed, and figures were created using Adobe Photoshop CS5 Extended (Adobe Systems Inc, San Jose, CA).

3. Results

3.1. Two homologues of human LIS1 in N. crassa

A blast search of the Neurospora database using the human LIS1 yielded two paralogues, the *lis1-1* and *lis1-2* genes. At the gene level, a sequence alignment with T-Coffee of the primary nucleotide sequences encoding LIS1-1 and LIS1-2 (Supplementary Fig. 1A) showed that despite the high homology in the coding region (>98%), a high level of divergence in the 5′- and 3′-non-coding and regulatory regions in each gene (Supplementary Fig. 1B and C). Furthermore, the genes encoding these two proteins are located far away from each other in the *N. crassa* genome and have an opposite strandness (Fig. 1A). This all indicates that the *lis1-1* and *lis1-2* paralogues were likely derived from duplication of a common ancestor.

The *N. crassa* paralogues LIS1-1 and LIS1-2 share about 98% amino acid sequence identity with each other, and when compared to human Lis1, LIS1-1 is the closest in homology (Fig. 1B). The predicted domains for LIS1-1 and LIS1-2 are shown in Fig. 1C, at the N-terminus, both had a LisH alpha-helical domain, followed by a coiled-coil motif that is lacking in LIS1-2 and seven WD40 repeats domains in the C-terminal (Fig. 1C).

3.2. Localization and dynamics of LIS1-1 and LIS1-2

LIS1-1 was tagged with GFP under its own promoter and under control of the *ccg-1* promoter, while LIS1-2 was just labeled under control of the *ccg-1* promoter (Fig. 2A and B; Supplementary Movie S1 and Movie S2). We did not find any difference in the expression of LIS1-1 with either promoter (data not shown). However, LIS1-2

Fig. 1. Comparison of *N. crassa* LIS1-1 and LIS1-2 with human LIS1. (A) Localization of *lis1-1* and *lis1-2* in the *N. crassa* genome, *lis1-1* is in 3′ to 5′ direction and *lis1-2* in 5′ to 3′. (B) Human Lis1, *N. crassa* LIS1-1 and LIS1-2 protein sequences (C) diagram of the different protein domains.

seems to be less abundant than LIS1-1 (Fig. 2B). LIS1-1-GFP and LIS1-2-GFP were distributed unevenly through different regions of the hypha. Single fluorescent particles could be seen traveling in the subapical region; as these particles reached the apex, they lined up forming prominent short filament-like structures (Fig. 2A and B). The accumulation of LIS1-1-GFP and LIS1-2-GFP reached their maximum density at the hyphal tip (Fig. 2A, 2B). These fluorescent structures moved exclusively in an anterograde fashion following the microtubular network (See kymograps in Fig. 2G, H). The resulting filament-like structures of LIS1-1-GFP and LIS1-2-GFP were arranged parallel to the cell growth axis which is the principal orientation of Mts in that region. As is the case for Mts, the filament-like structures seem to enter the Spk and traverse it (Fig. 2A and B). The fluorescence of LIS1-1-GFP or LIS1-2-GFP was not associated with nuclei or other organelles (Fig. 2A and B) and there was no fluorescence in old parts of the colony. LIS1-1-GFP filaments moved at $0.5 \pm 0.1\ \mu m\ s^{-1}$ (mean ± standard deviation) ($n = 30$), faster than the hyphal elongation rate ($0.2\ \mu m\ s^{-1}$). FRAP experiments corroborated the faster displacement rate of LIS1-1-GFP (data not shown), indicating that the fluorescent particles move independently of the cytoplasmic bulk flow.

To observe the interaction of LIS1-1 with Mt motor proteins, we conducted a co-expression experiment tagging LIS1-1 with mChFP and dynein (dynein light intermediate chain-DLIC), dynactin ($p150^{GLUED}$ subunit) or conventional kinesin (kinesin-1) with GFP. Dynein and dynactin formed similar short filament like structures

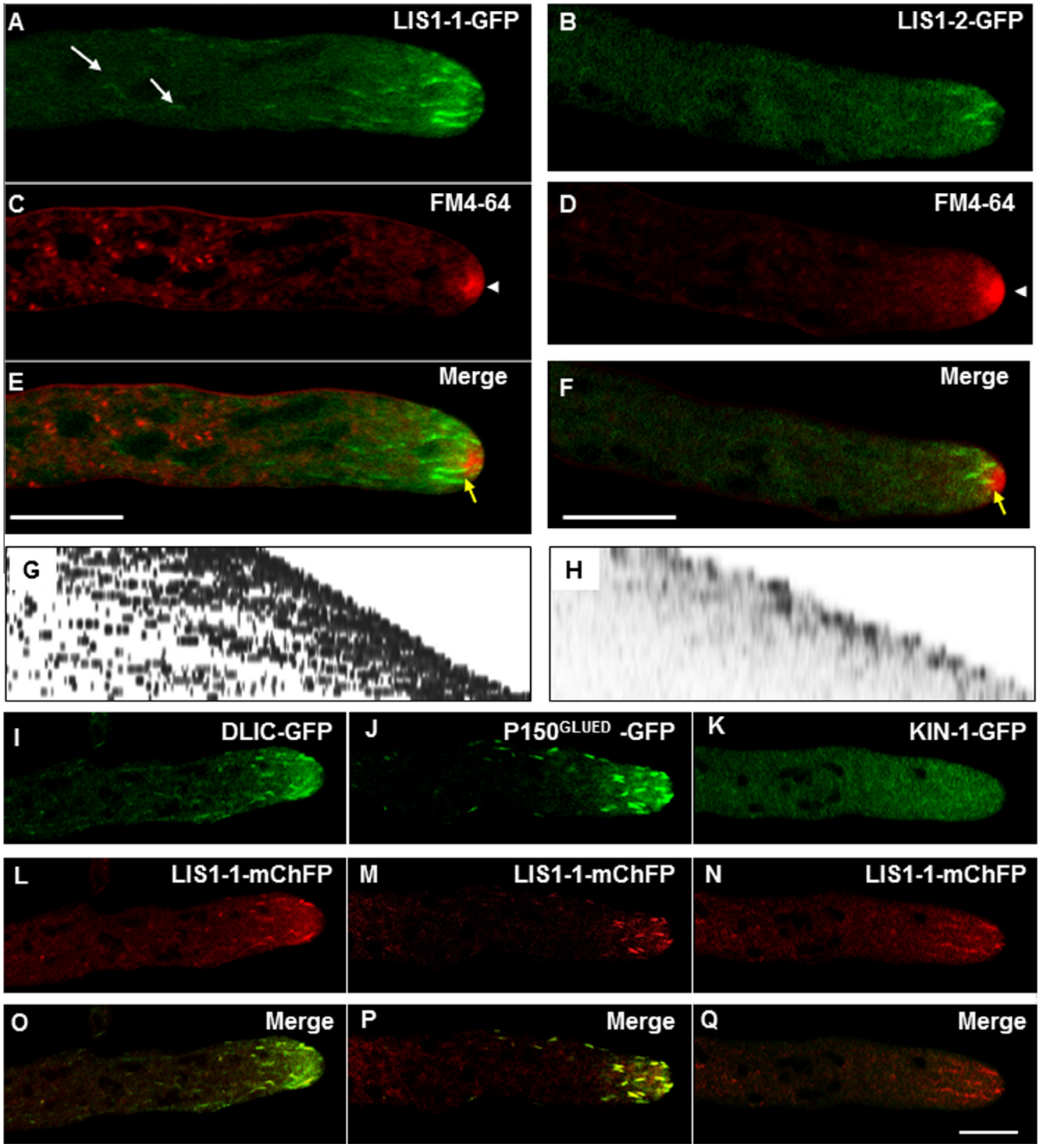

Fig. 2. Localization of LIS1-1 and LIS1-2 in mature hyphae and co-expression of LIS1-1 with three Mt motor proteins. (A) Short filament-like structures of LIS1-1-GFP, white arrows show small segments of LIS1-1-GFP in the subapex. (B) Short filament-like structures of LIS1-2-GFP. (C) and (D) Endomembranes stained with FM4-64 show the Spk (white arrowheads). (E) Merge of (A) and (C) yellow arrow shows how the short filament-like structures of LIS1-1-GFP accumulate in the apical region and traverse the Spk. (F) Merge of (B) and (D). (G) LIS1-1-GFP kymograph. (H) LIS1-2-GFP kymograph. (I) Dynein light intermediate chain (DLIC-GFP), (J) dynactin ($p150^{GLUED}$-GFP) and (K) conventional kinesin (KIN-1-GFP). (L), (M) and (N) LIS1-1-mChFP. (O) Merge of DLIC-GFP and LIS1-1-mChFP. (P) Merge of $p150^{GLUED}$-GFP and LIS1-1-mChFP. (Q) Merge of KIN-1-GFP and LIS1-1-mChFP. Optical slice of 0.9 μm. Scale bar = 10 μm. (For interpretation of the references to color in this figure legend, the reader is referred to the web version of this article.)

such as LIS1-1 and LIS1-2. KIN-1-GFP was distributed in a gradient from the very tip of the hypha, it was spread in the cytoplasm and it was not possible to observe single kinesin 1 molecules moving individually. We found that LIS1-1-mChFP co-localized fully with DLIC-GFP (dynein) and $p150^{GLUED}$-GFP (dynactin) but there was no co-localization with KIN-1-GFP (Fig. 2O–Q).

3.3. LIS1-1 and LIS1-2 interaction with Mts

LIS1-1-GFP was co-expressed in a strain having its β-tubulin labeled with –mChFP. LIS1-1-GFP decorated the Mts plus end in the apical dome (Fig. 3A; Supplementary Movie S3). We conducted a Mt-depolymerizing experiment with a sublethal concentration

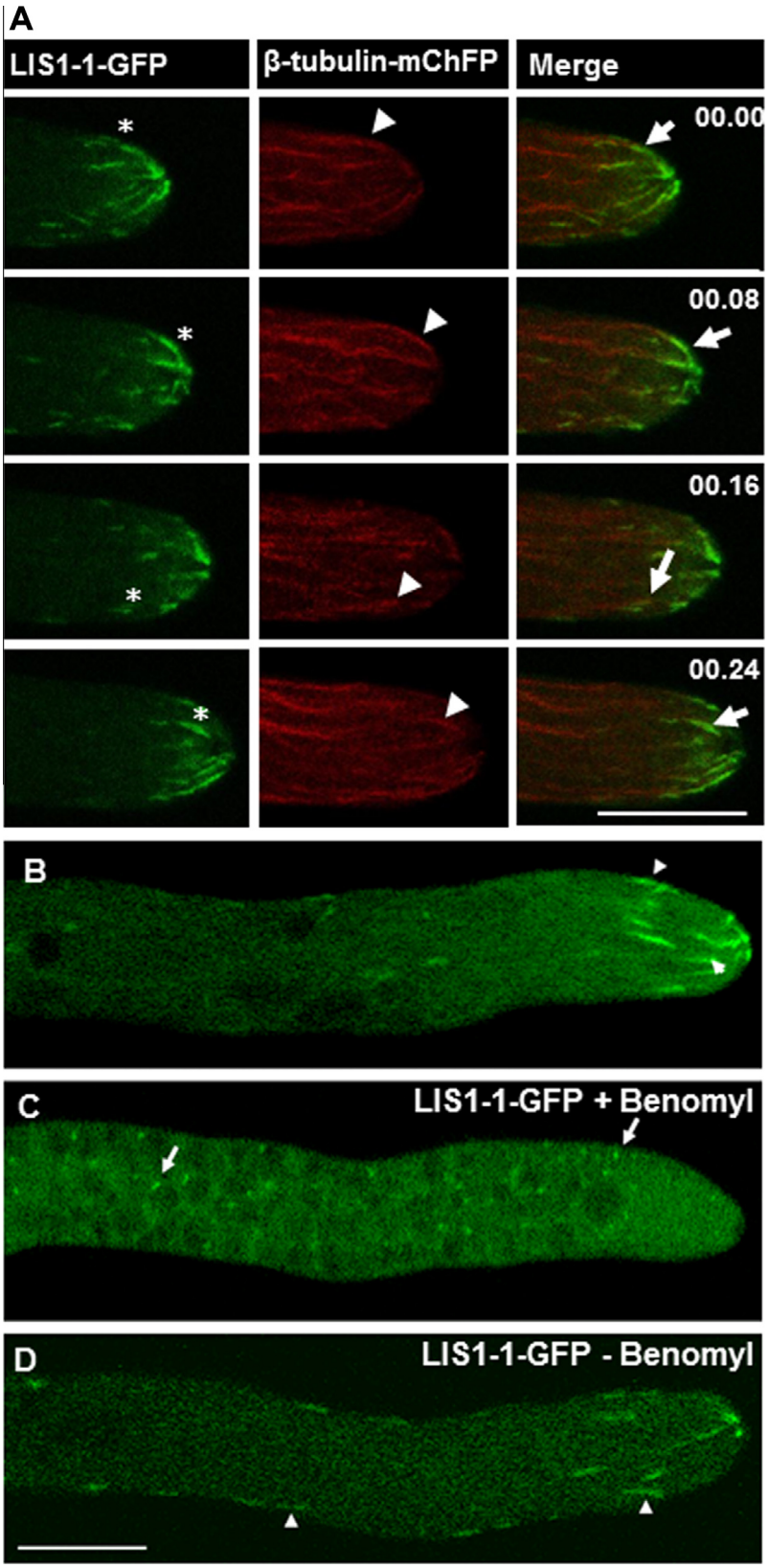

Fig. 3. Association of LIS1-1-GFP with Mts. (A) Co-expression of β-tubulin-mChFP and LIS1-1-GFP. (B)–(D) Effect of Mt dissociation on the localization LIS1-1-GFP. (B) Before benomyl treatment; (C) After 2 h treatment with 2.5 μg ml^{-1} benomyl; (D) Two hours after removal of benomyl. Benomyl treatment disperses the filament-like structures (arrowheads) into small fluorescent spots (arrows). Optical slice of 0.9 μm. Scale bar = 10 μm.

(2.5 μg ml^{-1}) of benomyl (Ramos-García et al., 2009) applied to the strains harboring LIS1-1-GFP and LIS1-2-GFP. Before benomyl treatment, we observed the filament-like fluorescent structures in the apical dome (Fig. 3B). After 2-h benomyl exposure, there were small disorganized fluorescent spots in the subapical region close to the nuclei (Fig. 3C). Two hours after washing out the

benomyl, the LIS1-1-GFP filaments were recovered (Fig. 3D). Similar results were observed with LIS1-2-GFP (not shown).

3.4. Mt motor protein affected LIS1-1 dynamics

LIS-1-GFP was expressed in strains with defects in motor proteins namely ropy-1 mutant (point mutation in *ro-1* FGSC4352 (dynein heavy chain)); ropy-3 mutant (point mutation in *ro-3* FGSC3 ($p150^{GLUED}$ subunit of dynactin)) and a deletion mutant of *kin-1* NRM104B. In the ropy-1 and ropy-3 mutants no filament-like structures were formed, fluorescence was dispersed in the cytoplasm and just small fluorescent spots were formed around the nuclei (Fig. 4), in the Δ*kin-1* mutant, there were less LIS1-1-GFP short filaments, but they were not affected in localization or movement (Fig. 4).

3.5. The LIS1 mutants

We characterized the Δ*lis1-1*, Δ*lis1-2* and the Δ*lis1-1*;Δ*lis1-2* double mutant of *N. crassa*. Growth rates of the Δ*lis1-1* mutant and the Δ*lis1-1*;Δ*lis1-2* double mutant were 62% and 75% less than WT, respectively (Figs. 5A, B, D, 6A). In contrast, the Δ*lis1-2* mutant had the same growth rate as the WT (Figs. 5C, 6A). To observe the effect of the increased expression of LIS1-2 in the Δ*lis1-1* mutant, we used the strain that had the LIS1-2-GFP (we used a strain expressing LIS1-2-GFP under the *ccg-1* promoter that is constitutive and increases the expression in addition to the endogenous levels of LIS1-2), we observed that the colony phenotype was not reverted to that of WT, but the growth rate increased from 0.05 ± 0.02 μm s^{-1} to 0.15 ± 0.03 μm s^{-1} (mean ± standard deviation) ($n = 11$; $p < 0.05$). Branching rate in Δ*lis1-1* mutant and Δ*lis1-1*;Δ*lis1-2* double mutant were 3-fold higher than the WT ($p < 0.05$; $n = 30$), and the LIS1-2 mutant showed a branching rate similar to that of WT (Figs. 5E–H, 6C).

To observe the apical organization of the Spk in the Δ*lis1-1* mutant, Δ*lis1-2* mutant and Δ*lis1-1*;Δ*lis1-2* double mutant, we stained the cells with FM4-64. We observed that Δ*lis1-1* mutant and Δ*lis1-1*;Δ*lis1-2* double mutant showed hyphae with smaller (Δ*lis1-1* 2.5 ± 0.2 μm [mean ± standard deviation]; $n = 15$, Δ*lis1-1*;Δ*lis1-2* 1.3 ± 0.2 μm; $n = 13$, WT 3.2 ± 0.3 μm; $n = 10$; $p < 0.05$) and less stable Spk (Fig. 5J–L; see Supplementary Movie S4) and also presented meandering growth (Fig. 5J, L, N, P). There was no observable difference between the Δ*lis1-2* mutant and the WT strain (Fig. 5I, K, M, O).

Conidia production was affected in all *lis1* mutants, the Δ*lis1-1*;Δ*lis1-2* double mutant had the strongest effect with 99% conidial production reduction (Fig. 6C). The biomass production was reduce in all mutants, we made the biomass production measurements by triplicate (Fig. 6D).

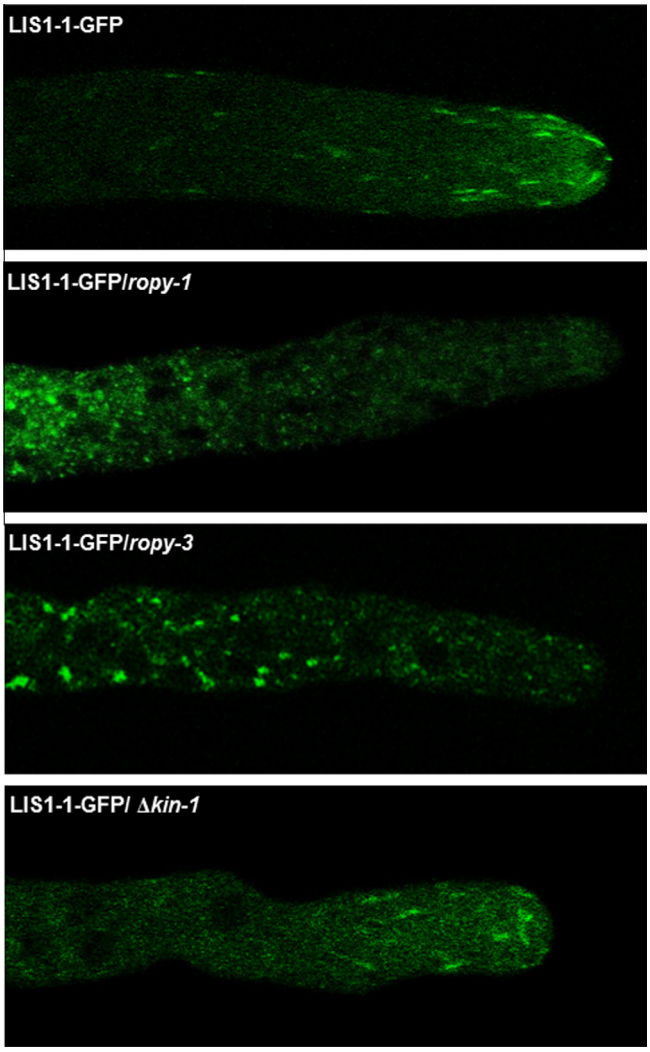

Fig. 4. Distribution pattern of LIS1-1-GFP in mutants deficient in motor proteins. Dynein heavy chain mutant (*ropy*-1), dynactin $p150^{GLUED}$ mutant (*ropy-3*), and conventional kinesin mutant (Δ*kin-1*). Note: the large black spots in the cytoplasm correspond to the profile of nuclei.

3.6. Lis1, Mts and dynein/dynactin complex distribution in the Lis1 mutants

To observe any interaction between both LIS1, we labeled LIS1-2-GFP in the Δ*lis1-1* mutant and LIS1-1-GFP in the Δ*lis1-2* mutant (Fig. 7A–C). We observed that there was no effect in the filament-like structures of LIS1-1-GFP in the Δ*lis1-2* mutant, however there were less LIS1-2-GFP filament-like structures in the Δ*lis1-1* mutant (Fig. 7C; Supplementary Movie S5 and S6). We also labeled Mts in both Δ*lis1-1* and Δ*lis1-2* mutants (Fig. 7D–F). The microtubular cytoskeleton was strongly affected in the Δ*lis1-1* mutant compared with the Δ*lis1-2* mutant (Fig. 7F; Supplementary Movie S8) and WT strain (Fig. 7D). Mts were fewer, more curved, and they seemed to be organized in bundles and just a few reached the apex (Fig. 7E; Fig. 8; Supplementary Movie S7). The decrease in Mt number in the Δ*lis1-1* mutant is consistent with the finding of less LIS1-2-GFP filament-like structures in this mutant.

Dynein and dynactin, tagged with GFP, were present as filaments moving toward the apex and both accumulated in the very tip of the hypha (Fig. 9A, C). In the Δ*lis1-1* mutant, most of the dynein and dynactin did not form filaments, but was present as fluorescence spots distributed along the hyphae (Fig. 9B, D). A few short filaments were observed but they did not reach the apical dome (Fig. 9B, D; white arrows).

3.7. Nuclei and mitochondria distribution in lis1 mutants

In the Δ*lis1-1* mutant nuclear morphology and distribution was slightly altered in comparison with the WT strain. There were similar number of nuclei in the subapical region, but the exclusion zone was smaller (Fig. 10; Supplementary Movie S9). The vast majority of nuclei in this mutant were spherical although there were some examples of slightly oval or pear-shaped nuclei (Fig. 10). In the WT strain, nuclei were uniformly distributed throughout the subapical region with an apical exclusion zone of 12 μm ($n = 30$) (Fig. 10). The majority of the nuclei showed a

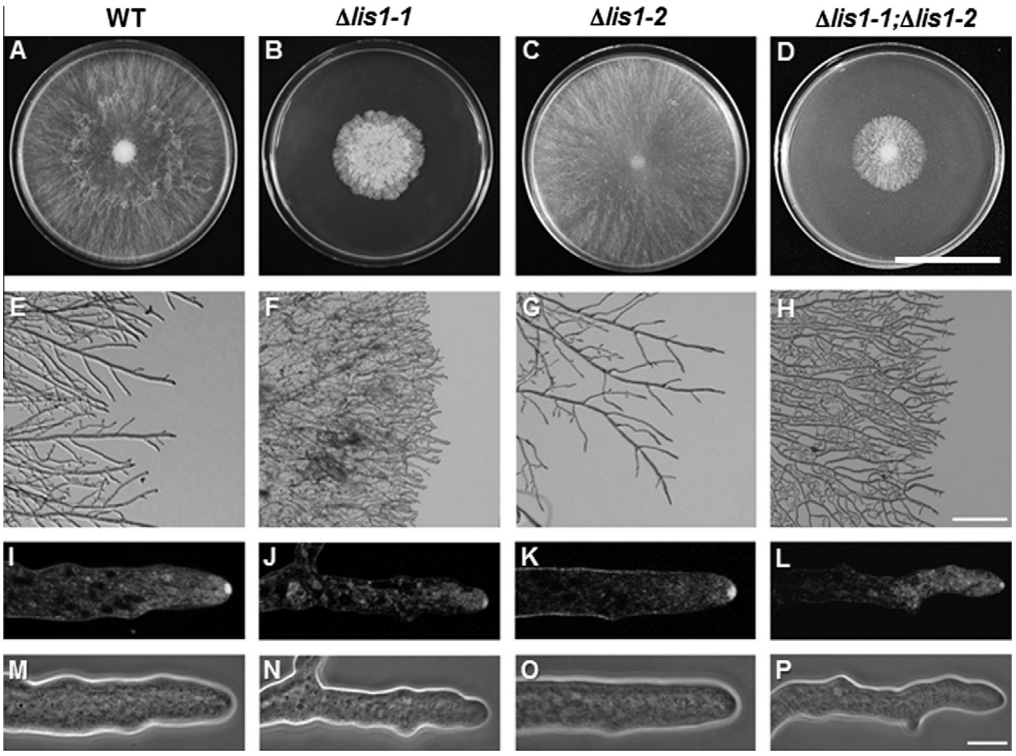

Fig. 5. Morphology of *N. crassa* WT, Δ*lis1-1* mutant, Δ*lis1-2* mutant and a Δ*lis1-1*;Δ*lis1-2* double mutant. First row shows the colonial morphology; scale bar = 5 cm. Second row shows the edges of the colonies at higher magnification; scale bar = 100 μm. Third row shows confocal microscopy of hyphae stained with FM4-64 to observe the features of the Spk in the WT strain and the three mutants. Optical slice of 0.9 μm; scale = 10 μm. Fourth row shows phase contrast images of the respective strains. Arrows indicates the Spk. Scale bar = 10 μm.

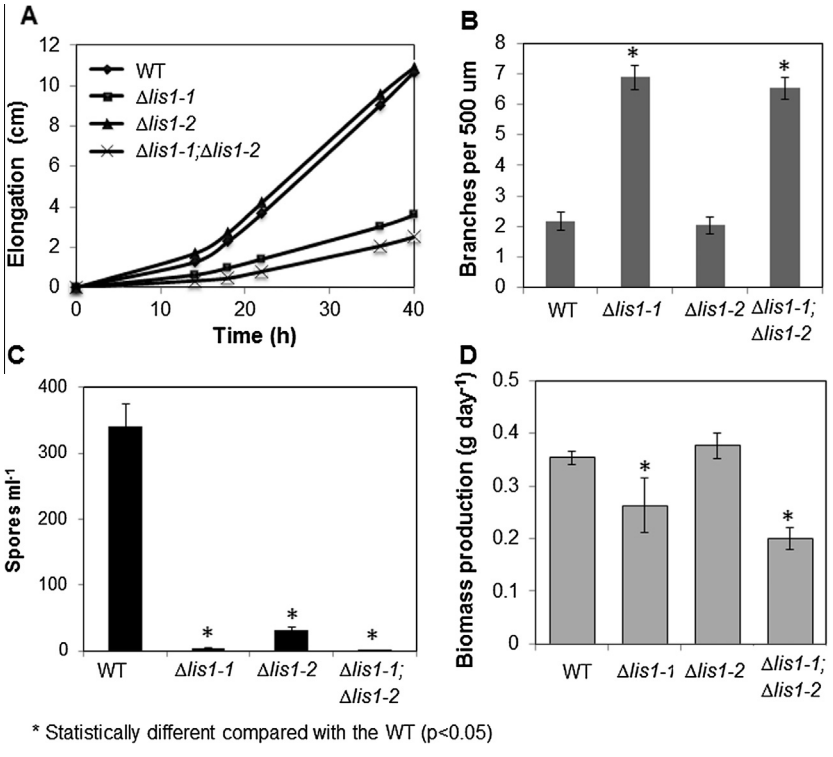

Fig. 6. Growth kinetics of *lis1* mutants. (A) Radial growth of colonies in WT (•), Δ*lis1-1* (■), Δ*lis1-2* mutant (▲), and Δ*lis1-1*;Δ*lis1-2* double mutant (x). (B) Branching rate per 500 μm of hyphal length, (C) conidiation rate (conidia ml^{-1}) and (D) biomass production (mg d^{-1}). Error bars = confidence interval at 95%.

pyriform shape, they were elongated and oriented parallel to the growth axis (Fig. 10).

As mitochondria displacement is Mt dependent (Fuchs et al., 2002), we labeled mitochondria with Syto® Red and observed their distribution in the apical and subapical region of hyphae of *N. crassa*. In the Δ*lis1-1* mutant and the Δ*lis1-1*;Δ*lis1-2* double mutant, mitochondria accumulated in the subapical region, while the Δ*lis1-2* mutant and the WT strain their mitochondria clustered

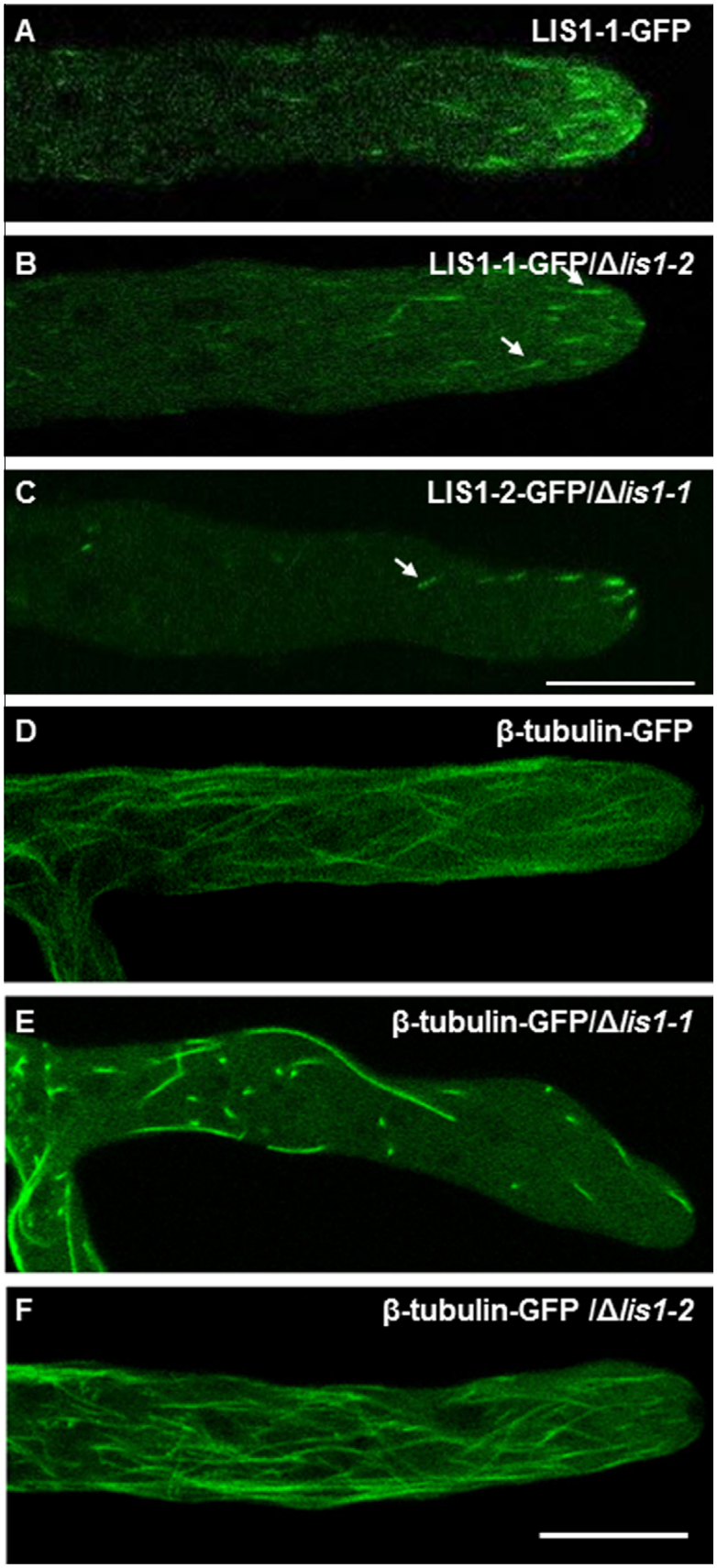

Fig. 7. Distribution of LIS1-1 and LIS1-2 and Mt organization in the respective *lis1* mutants. (A) LIS1-1-GFP in WT strain. (B) LIS1-1-GFP in Δ*lis1*-2 mutant (C) LIS1-2-GFP in Δ*lis1-1* mutant. (D) β-tubulin-GFP in WT, (E) β-tubulin-GFP in Δ*lis1-1* mutant, and (F) β-tubulin-GFP in Δ*lis1*-2 mutant. Optical slice of 0.9 μm. Scale bar = 10 μm.

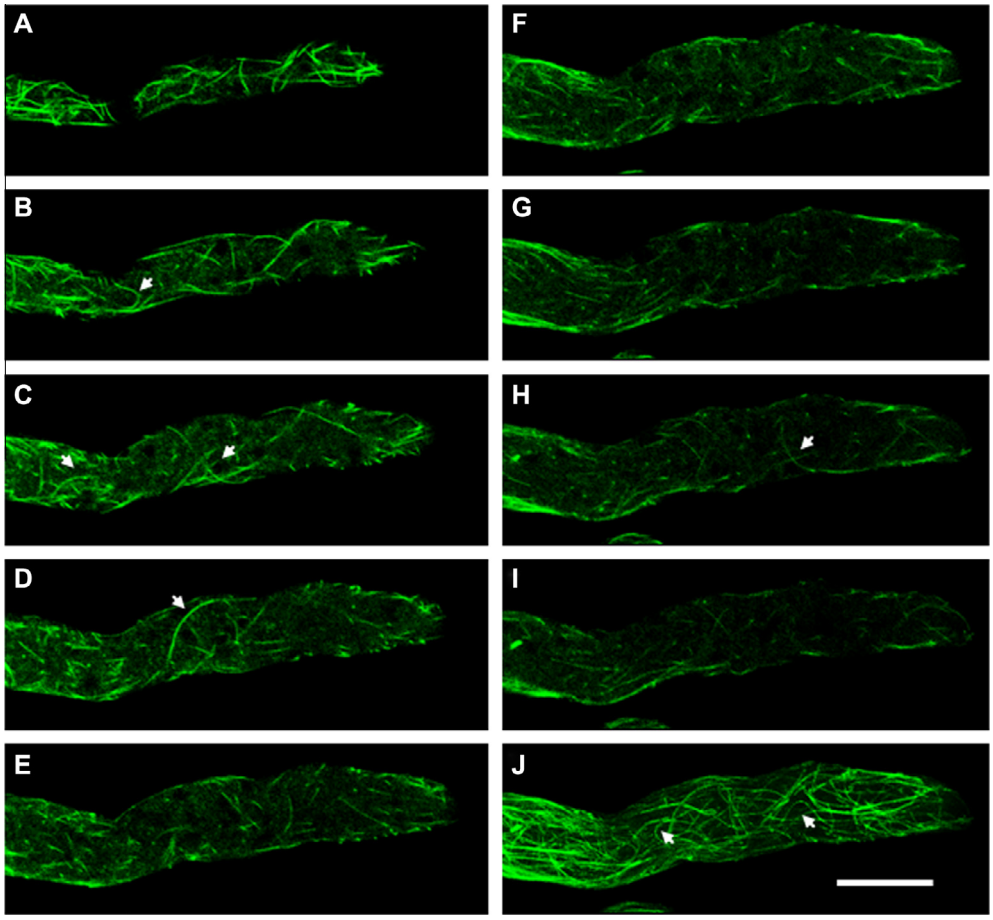

Fig. 8. Microtubular cytoskeleton 3D reconstruction in the Δ*lis1-1* mutant. (A)–(I) z-stacks, (J) Maximum projection. Scale bar = 10 μm.

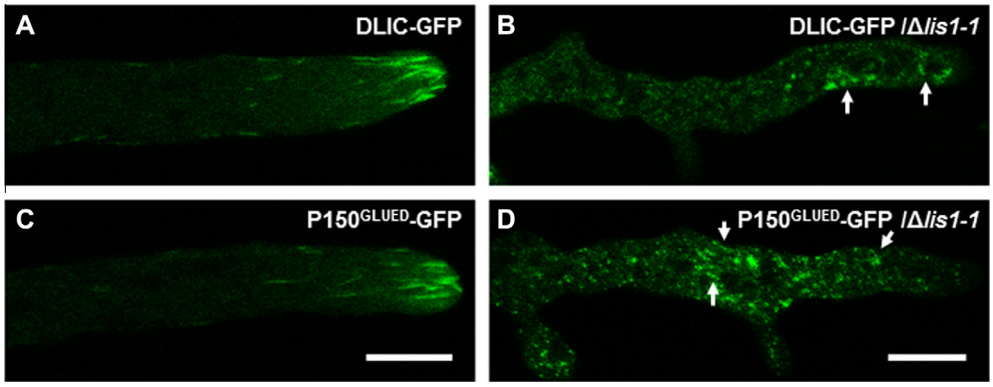

Fig. 9. Distribution of Mts motor proteins in the Δ*lis1-1* mutant. Dynein heavy chain mutant (DLIC-GFP) (A) in the WT strain, (B) in the Δ*lis1-1* mutant. Dynactin subunit $P150^{GLUED}$ (C) in the WT strain, (D) in the Δ*lis1-1* mutant. Scale bar = 10 μm.

in the apical dome (Fig. 11A). When we compared the distribution of mitochondria and Mts, we observed that abnormal organization of Mts in the Δ*lis1-1* mutant appeared to contribute to the lack of mitochondria in the very tip of the hypha (Fig. 11B; Supplementary Movie S10 and S11).

4. Discussion

4.1. Homologues of human LIS1 in N. crassa

We have found that LIS1, a Mt plus end protein known to be present in a great variety of organisms, is also present in *N. crassa*. However, unlike other organisms, this fungus has two versions of LIS1 in its genome, described herein as LIS1-1 and LIS1-2. The presence of paralogues in *N. crassa* is surprising because this fungus lacks repetitive genomic sequences (Galagan et al., 2003). The *lis1-1* and *lis1-2* genes are located far away from each other in the *N. crassa* genome and have an opposite strandness. This suggests that the *lis1-1* and *lis1-2* paralogues were derived from the duplication of a common ancestor. There are other examples of Ascomycetes that have two Lis1 such as *Podospora anseriana*, *Neurospora tetrasperma*, *Sordaria macrospora* among others.

The structure of human Lis1 has been solved by X-ray crystallography, unveiling two structured regions connected by an unstructured loop (Kim et al., 2004; Tarricone et al., 2004). At the

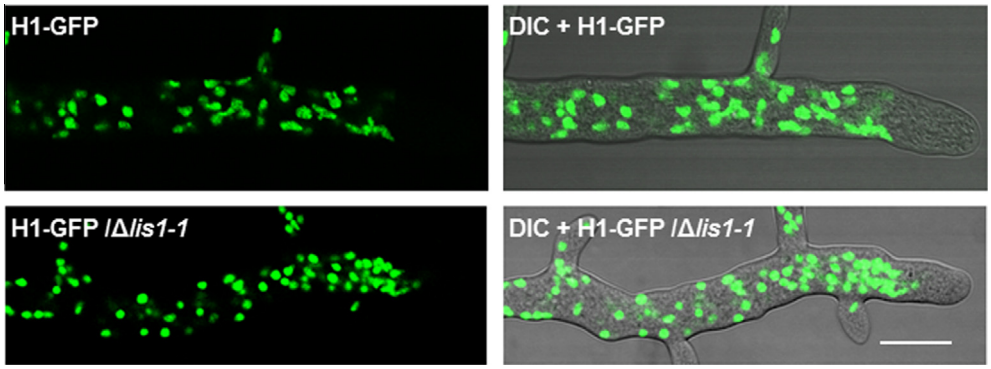

Fig. 10. Nuclear distribution in the WT strain and the Δ*lis1-1* mutant. DIC- Differential interference contrast microscopy image. Scale bar = 10 μm.

N-terminus, human Lis1 has a LisH alpha-helical domain, followed by a coiled-coil motif. After an unstructured loop, the C-terminal region folds into a beta propeller domain, composed by seven WD40 repeats. Experimental evidence indicates that the LisH domain is essential for *in vivo* homodimerization (Kim et al., 2004; Mateja et al., 2006), and contains a binding site for known LIS1 protein interactors, such as Nde1 (Derewenda et al., 2007). Both the LisH domain and the coiled-coil motif are known structural mediators of protein–protein interactions and mass spectrometry evidence indicates that the LisH domain and its flanking regions in LIS1 are rich in post-translational modifications (PTMs), suggesting functional regulation (http://www.phosphosite.org/proteinAction.do?id=8064&showAllSites=true). This is relevant because the sequence forming the coiled-coil in LIS1 is present in LIS1-1 but absent in LIS1-2, suggesting differential protein interactors between the two *N. crassa* paralogues, possibly regulated by the various PTM reported so far. Overall, despite the high amino acid homology between human LIS1 and *N. crassa* LIS1-1 and LIS1-2, the absence of the coiled-coil motif in LIS1-2 suggests that its function or regulation may be distinct from that of LIS1-1.

The database Phosphosite reports several Lys acetylation and ubiquitination sites, and one phosphorylation site on a Ser, a Thr and a Tyr within the LisH and coiled-coil domains of LIS1 (http://www.phosphosite.org/proteinAction.do?id=8064&showAllSites=true). This observation is interesting in light of the higher expression levels of LIS1-1, compared to LIS1-2 in *N. crassa*, suggesting context-dependent regulated functions. Lys ubiquitylation is a PTM that typically tags a protein for degradation by the proteasome and the LisH domain in LIS1 is thought to regulate the protein's half-life (Gerlitz et al., 2005). Our data therefore suggests the hypothesis that the lower levels of LIS1-2, compared to LIS1-1, might be regulated by the proteasome. In support of this hypothesis, the recently published draft of the human proteome found that LIS1 is expressed at low levels in most human tissues (Kim et al., 2014).

4.2. The lack of LIS1 in N. crassa

In contrast to the LIS1 of *Ustilago maydis* (Valinluck et al., 2010), deletion mutants of the two LIS1 homologs of *N. crassa* showed that neither one is essential for viability. This is similar to other fungi where LIS1 is also dispensable (Xiang et al., 1995; Lee et al., 2003; Sheeman et al., 2003; Efimov et al., 2006). In *U. maydis* also the two genes encoding for dynein heavy chain *dyn1* and *dyn2* are essential for cell survival (Straube et al., 2001). LIS1-1 does not seem to be involved in nuclear migration directly as it is in other eukaryotes, however, we demonstrate that LIS1-1 plays a role in hyphal morphogenesis and Mt organization. There were dramatic alterations of cell morphology in *N. crassa* lacking LIS1-1 but not in cells devoid of LIS1-2, similar to the normal cell morphology of *Saccharomyces cerevisiae* pac1 mutants (Lee et al., 2003). The Δ*nudF* mutant of *A. nidulans* forms small colonies due to slow growth but hyphae do not exhibit altered cell polarity or morphology (Efimov et al., 2006). The colony phenotype of Δ*lis1-1* is very similar to the phenotype of the ropy mutants (dynein/dynactin complex) that result in curled hyphal tips or spiral hyphae (Plamann et al., 1994; Inoue et al., 1998), suggesting also a role in normal hyphal morphology. Presumably, LIS1-1-lacking hyphae exhibit abnormal hyphal growth due to deficient Mt function, which probably results in altered transport of vesicles to growth regions.

4.3. LIS1-1 and LIS1-2 proteins localize at the Mt plus ends

In contrast to *A. nidulans*, we did not observe retrograde movement of LIS1-1-GFP and LIS1-2-GFP (Han et al., 2001). Both LIS1-1-GFP and LIS1-2-GFP form filament-like structures that migrate rapidly in anterograde direction and concentrate in the hyphal tip. The dynamic behavior of both LIS1 proteins is basically identical to that exhibited by dynein and dynactin in *A. nidulans* (Zhang et al., 2003; Yao et al., 2012) and *N. crassa* (Mouriño-Pérez unpublished).

Both LIS1-1 and LIS1-2 were indeed located at the ends of the Mts as is true in other fungi such as *A. nidulans* (Han et al., 2001) and *U. maydis* (Lenz et al., 2006), LIS1 and the dynein and dynactin complex has been found to localize to the distal ends of Mts near the cell periphery (Vaughan et al., 1999; Valetti et al., 1999; Han et al., 2001; Lee et al., 2003). These observations suggest that the location of these proteins is conserved between filamentous fungi and mammals. Treatment with sub-lethal concentration of the Mt depolymerizing drug benomyl caused the filament-like structures of LIS1-1 and LIS1-2 disappeared, as was the case in *A. nidulans*. The fluorescent particles were concentrated in the subapex similar to the behavior of another +TIP protein *N. crassa* MTB-3 a EB1 homologue in benomyl-treated cells (Mouriño-Pérez et al., 2013) and CLIP-170 (Perez et al., 1999; Dragestein et al., 2008) and APC (Mimori-Kiyosue et al., 2000a, 2000b) from mammals.

LIS1 affects Mt dynamics and is required for organization of the Mt cytoskeleton (Straube et al., 2003). In wild type cells of *U. maydis*, Mts grow toward the cell tip and do not curve around the tip or form unusual structures (Steinberg et al., 2001). However, cells lacking LIS1-1 contain just a few Mts, which bend at the cell tips and grow backward and are undulated or form coils perpendicular to the long axis of the cell (Valinluck et al., 2010). In contrast, the number and length of Mts were not altered in *A. nidulans NudF* or *S. cerevisiae pac1* mutants. Microtubular changes in LIS1-1 deletion mutant were similar to those in the dynein and dynactin mutants in *A. nidulans*, *N. crassa* and *Ashbya gossypii* that exhibit undulated

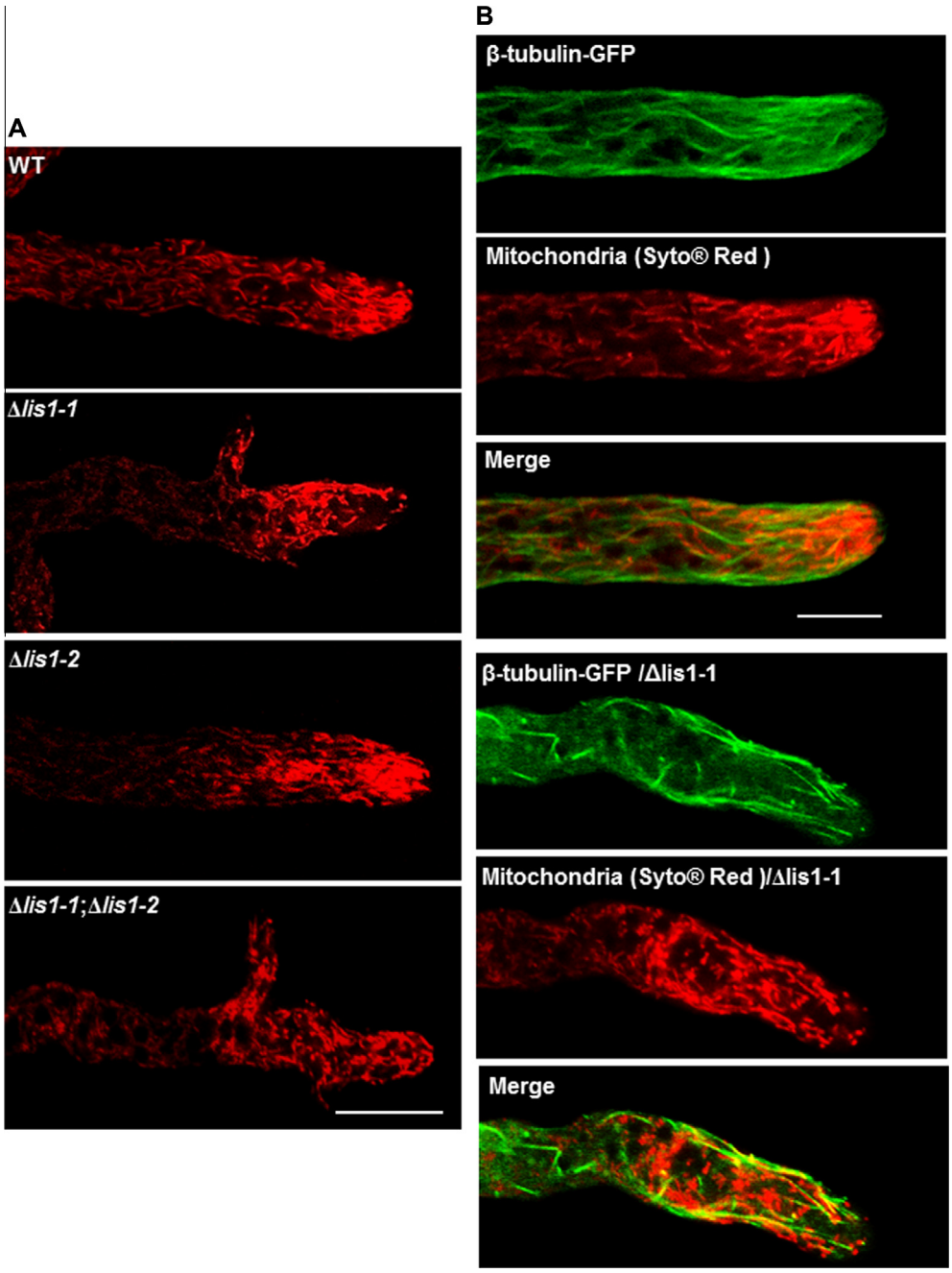

Fig. 11. Mitochondrial distribution in *lis1* mutants. (A) Mitochondria labeled with SYTO® Red in the WT, Δ*lis1-1* and Δ*lis1*-2 mutants. (B) Mitochondria labeled with SYTO® Red and Mt labeled with β-tubulin-GFP in WT and Δ*lis1-1* mutant. Optical slice of 0.9 μm. Scale bar = 10 μm.

or aberrant Mts (Tinsley et al., 1996; Minke et al., 1999; Riquelme et al., 2002; Alberti-Segui et al., 2001; Liu et al., 2003; Uchida et al., 2008).

4.4. Formation of LIS1 short filaments

Two different mechanisms have been proposed to explain the accumulation of Mt plus-end proteins at the plus-ends of Mts, one is treadmilling that involves the association of proteins with the very end of the growing Mt, either during polymerization (Diamantopoulos et al., 1999) or by recognition of a specific target in Mt distal end and subsequent release from a part of the Mt without the target. Examples of proteins associated by treadmilling are EB1 (MTB-3 in *N. crassa*; Mouriño-Pérez et al., 2013) and CLIP-170 (Rickard and Kreis, 1991; Choi et al., 2002; Vaughan et al., 2002). The other mechanism is called the sliding model in which proteins associate with Mts along their entire length, and travel, by motor proteins, toward the Mt plus end. During this travel, they become associated leading to the formation of filament- or comet-like structures at the cell periphery (Galjart and Perez, 2003) just as the filament-like structures produced by LIS1-1-GFP and LIS1-2-GFP (Fig. 12). The sliding model was first proposed for APC (Ademomatous polyposis coli) (Bienz, 2002).

4.5. LIS1 and the dynein/dynactin complex

As in other studies, *N. crassa* LIS1-1 seems to regulate dynein activity (Faulkner et al., 2000; Smith et al., 2000; Cockell et al.,

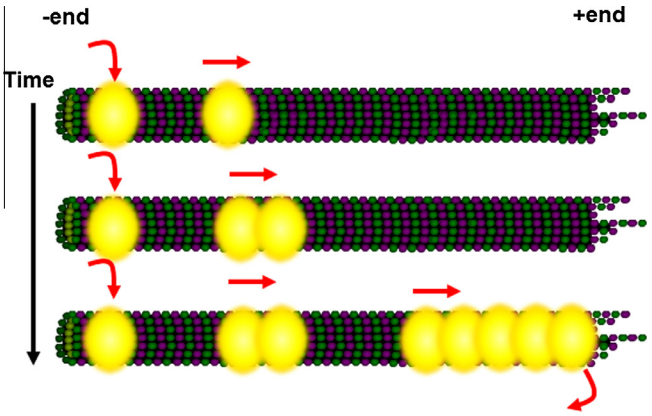

Fig. 12. Schematic model of LIS1-1 and LIS1-2 movement along Mts. LIS1 is recruited in basal parts of the hypha and slides in anterograde direction and it is becoming associated with other LIS1 molecules, forming short filaments-like structure in the Mts plus end. Modified from Galjart and Perez (2003).

2004; Zhang et al., 2003, 2010; Lansbergen et al., 2004; Mesngon et al., 2006; Yamada et al., 2008; McKenney et al., 2010; Huang et al., 2012; Egan et al., 2012). We provide evidence of the association between LIS1 and the dynein–dynactin complex, as indicted by the high colocalization between LIS1-1 and dynein and dynactin at the tip. Also, the depletion of dynein significantly decreased the amount of LIS1-1 at the hyphal apex. Our findings are consistent with the suggestion by Zhang et al. (2010) that LIS1-1, dynein and dynactin accumulates at the Mts plus-ends as part of the same complex. There is a regulatory effect of LIS1-1 on dynein/dynactin, as proposed that LIS1-1 serves as a "clutch" maintaining a stable connection between motor dynein and the plus-end of the Mts (Huang et al., 2012).

4.6. Deletion studies: LIS1-1 vs LIS1-2

The totally different phenotypes resulting from deletion of LIS-1-1 and/or LIS-1-2 clarified the relative importance of these paralogues. The Δ*lis-1-1* mutant grew very poorly and produced few conidia showing that LIS-1-2 could not compensate for the deletion of LIS-1-1, although the overexpression of LIS1-2 in a Δ*lis-1-1* mutant background resulted in a recovery of the growth rate. LIS-1-1 did compensate for the deletion of LIS-1-2 as this mutant exhibited no deficiency in growth or conidiation. As expected, the double mutation Δ*lis-1-1* and Δ*lis-1-2* led to very poor growth, proof of the functional essentiality of LIS1-1 and the dispensability of LIS1-2 in *N. crassa*.

Acknowledgments

This work was supported by grants from Consejo Nacional de Ciencia y Tecnología (Ciencia Basica-2010-133518 to R.R.M.P). We thank the Neurospora Functional Genomics project (NIH P01GM068087) and the Fungal Genetics Stock Center (FGSC, Kansas City, MO) for strains.

Appendix A. Supplementary material

Supplementary data associated with this article can be found, in the online version, at http://dx.doi.org/10.1016/j.fgb.2015.07.009.

References

Alberti-Segui, C., Dietrich, F., Altmann-Jöhl, R., Hoepfner, D., Philippsen, P., 2001. Cytoplasmic dynein is required to oppose the force that moves nuclei toward the hyphal tip in the filamentous ascomycete *Ashbya gossypii*. J. Cell Sci. 114, 975–986.

Barth, P.G., Mullaart, R., Stam, F.C., Sloof, J.L., 1982. Familial lissencephaly with extreme neopallial hypoplasia. Brain Dev. 4, 145–151.

Bienz, M., 2002. The subcellular destinations of APC proteins. Nat. Rev. Mol. Cell Biol. 3, 328–338.

Choi, J.H., Bertram, P.G., Drenan, R., Carvalho, J., Zhow, H.H., Zheng, X.F., 2002. The FKBP12-rapamycin associated protein (FRAP) is a CLIP-170 kinase. EMBO Rep 13, 13.

Cockell, M.M., Baumer, K., Gönczy, P., 2004. Lis-1 is required for dynein-dependent cell division processes in *C. elegans* embryos. J. Cell Sci. 117, 4571–4582.

Colot, H.V., Park, G., Turner, G.E., Ringelberg, C., Crew, C.M., Litvinkova, L., Weiss, R.L., Borkovich, K.A., Dunlap, J.C., 2006. A high-throughput gene knockout procedure for *Neurospora* reveals functions for multiple transcription factors. Proc. Natl. Acad. Sci. USA 103, 10352–10357.

Davis, R., 2000. *Neurospora*: Contributions of a Model Organism. Oxford University Press.

Derksen, J., Emons, A.M., 1990. Microtubules in tip growing systems. In: Heath, I.B. (Ed.), Tip Growth in Plant and Fungal Cells. Academic Press, San Diego.

Derewenda, U., Tarricone, C., Choi, W.C., Cooper, D.R., Lukasik, S., Perrina, F., Tripathy, A., Kim, M.H., Cafiso, D.S., Musacchio, A., Derewenda, Z.S., 2007. The structure of the coiled-coil domain of Ndel1 and the basis of its interaction with Lis1, the causal protein of Miller-Dieker lissencephaly. Structure 15 (11), 1467–1481.

Diamantopoulos, G.S., Prez, F., Goodson, H.V., Bateller, G., Melki, R., Kreis, T.E., Rickard, J.E., 1999. Dynamic localization of CLIP-170 to microtubule plus ends in coupled to microtubule assembly. J. Cell Biol. 144, 99–112.

Dieker, H., Edwards, R.H., ZuRhein, G., Chou, S.M., Hartman, H.A., Opitz, J.M., 1969. The lissencephaly syndrome. Birth Defects 5, 53–64.

Dobyns, W.B., 1989. The neurogenetics of lissencephaly. Neurol. Clin. 7 (1), 89–105.

Dobyns, W.B., Curry, C.J., Hoyme, H.E., Turlington, L., Ledbetter, D.H., 1991. Clinical and molecular diagnosis of Miller-Dieker syndrome. Am. J. Hum. Genet. 48 (3), 584–594.

Dragestein, K.A., van Cappellen, W.A., van Haren, J., Tsibidis, G.D., Akhmanova, A., Knoch, T.A., Grosveld, F., Galjart, N., 2008. Dynamic behavior of GFP-CLIP-170 reveals fast protein turnover on microtubule plus ends. J. Cell Biol. 180 (4), 729–737. http://dx.doi.org/10.1083/jcb.200707203.

Efimov, V.P., 2003. Roles of NUDE and NUDF proteins of *Aspergillus nidulans*: insights from intracellular localization and overexpression effects. Mol. Biol. Cell 14 (3), 871–888.

Efimov, V.P., Zhang, J., Xiang, X., 2006. CLIP-170 homologue and NUDE play overlapping roles in NUDF localization in *Aspergillus nidulans*. Mol. Biol. Cell 17 (4), 2021–2034.

Egan, M.J., Tan, K., Reck-Peterson, S.L., 2012. Lis1 is an initiation factor for dynein-driven organelle transport. J. Cell Biol. 197 (7), 971–982.

Faulkner, N.E., Dujardin, D.L., Tai, C.Y., Vaughan, K.T., O'Connell, C.B., Vallee, R.B., Wang, Y.I., 2000. A role for the lissencephaly gene LIS1 in mitosis and cytoplasmic dynein function. Nat. Cell Biol. 2, 784–791.

Fischer-Parton, S., Parton, R.M., Hickey, P.C., Dijksterhuis, J., Atkinson, H.A., Read, N.D., 2000. Confocal microscopy of FM4-64 as a tool for analysing endocytosis and vesicle trafficking in living fungal hyphae. J. Microsc. 198 (Pt 3), 246–259.

Freitag, M., Hickey, P.C., Raju, N.B., Selker, E.U., Read, N.D., 2004. GFP as a tool to analyze the organization, dynamics and function of nuclei and microtubules in *Neurospora crassa*. Fungal Genet. Biol. 41, 897–910.

Fuchs, F., Prokisch, H., Neupert, W., Westermann, B., 2002. Interaction of mitochondria with microtubules in the filamentous fungus *Neurospora crassa*. J Cell Sci. 115, 1931–1937.

Galagan, J.E., Calvo, S.E., Borkovich, K.A., Selker, E.U., Read, N.D., Jaffe, D., FitzHugh, W., Ma, L.J., Smirnov, S., Purcell, S., Rehman, B., Elkins, T., Engels, R., Wang, S., Nielsen, C.B., Butler, J., Endrizzi, M., Qui, D., Ianakiev, P., Bell-Pedersen, D., Nelson, M.A., Werner-Washburne, M., Selitrennikoff, C.P., Kinsey, J.A., Braun, E.L., Zelter, A., Schulte, U., Kothe, G.O., Jedd, G., Mewes, W., Staben, C., Marcotte, E., Greenberg, D., Roy, A., Foley, K., Naylor, J., Stange-Thomann, N., Barrett, R., Gnerre, S., Kamal, M., Kamvysselis, M., Mauceli, E., Bielke, C., Rudd, S., Frishman, D., Krystofova, S., Rasmussen, C., Metzenberg, R.L., Perkins, D.D., Kroken, S., Cogoni, C., Macino, G., Catcheside, D., Li, W., Pratt, R.J., Osmani, S.A., DeSouza, C.P., Glass, L., Orbach, M.J., Berglund, J.A., Voelker, R., Yarden, O., Plamann, M., Seiler, S., Dunlap, J., Radford, A., Aramayo, R., Natvig, D.O., Alex, L.A., Mannhaupt, G., Ebbole, D.J., Freitag, M., Paulsen, I., Sachs, M.S., Lander, E.S., Nusbaum, C., Birren, B., 2003. The genome sequence of the filamentous fungus *Neurospora crassa*. Nature 422, 859–868.

Galjart, N., Perez, F., 2003. A plus-end raft to control microtubule dynamics. Curr. Opin. Cell Biol. 15, 48–53.

Garvalov, B.K., Zuber, B., Bouchet-Marquis, C., Kudryashev, M., Gruska, M., Beck, M., Leis, A., Frischknecht, F., Bradke, F., Baumeister, W., Dubochet, J., Cyrklaff, M., 2006. Luminal particles within cellular microtubules. J Cell Biol. 174 (6), 759–765.

Gerlitz, G., Darhin, E., Giorgio, G., Franco, B., Reiner, O., 2005. Novel functional features of the Lis-H domain: role in protein dimerization, half-life and cellular localization. Cell Cycle 4 (11), 1632–1640.

Haimo, L.T., 1997. Ordering microtubules. Bioessays. 19 (7), 547–550.

Han, G., Liu, B., Zhang, J., Zuo, W., Morris, N.R., Xiang, X., 2001. The *Aspergillus* cytoplasmic dynein heavy chain and NUDF localize to microtubule ends and affect microtubule dynamics. Curr. Biol. 11 (9), 719–724.

Hattori, M., Adach, i.H., Tsujimoto, M., Arai, H., Inoue, K., 1994. Miller-Dieker lissencephaly gene encodes a subunit of brain platelet-activating factor acetylhydrolase [corrected]. Nature 370 (6486), 216–218 (Erratum in: Nature 1994 4;370(6488): 39).

Hickey, P.C., Jacobson, D., Read, N.D., Glass, N.L., 2002. Live-cell imaging of vegetative hyphal fusion in *Neurospora crassa*. Fungal Genet. Biol. 37 (1), 109–119.

Hirokawa, N., 1998. Kinesin and dynein superfamily proteins and the mechanism of organelle transport. Science 279, 519–526.

Howard, R.J., Aist, J.R., 1980. Cytoplasmic microtubules and fungal morphogenesis: ultrastructural effects of methyl benzimidazole-2-ylcarbamate determined by freeze-substitution of hyphal tip cells. J. Cell Biol. 87 (1), 55–64.

Huang, J., Roberts, A.J., Leschziner, A.E., Reck-Peterson, S.L., 2012. Lis1 acts as a "Clutch" between the ATPase and microtubule-binding domains of the dynein motor. Cell 150, 975–986.

Inoue, S., Turgeon, B.G., Yoder, O.C., Aist, J.R., 1998. Role of fungal dynein in hyphal growth, microtubule organization, spindle pole body motility and nuclear migration. J. Cell Sci. 111, 1555–1566.

Izumi, K., Kuratsuji, G., Ikeda, K., Takahash, i.T., Kosaki, K., 2007. Partial deletion of LIS1: a pitfall in molecular diagnosis of Miller-Dieker syndrome. Pediatr. Neurol. 36 (4), 258–260.

Kim, M.H., Cooper, D.R., Oleksy, A., Devedjiev, Y., Derewenda, U., Reiner, O., Otlewski, J., Derewenda, Z.S., 2004. The structure of the n-terminal domain of the product of the lissencephaly gene lis1 and its functional implications. Structure 12, 987.

Kim, M.S., Pinto, S.M., Getnet, D., Nirujogi, R.S., Manda, S.S., Chaerkady, R., Madugundu, A.K., Kelkar, D.S., Isserlin, R., Jain, S., Thomas, J.K., Muthusamy, B., Leal-Rojas, P., Kumar, P., Sahasrabuddhe, N.A., Balakrishnan, L., Advani, J., George, B., Renuse, S., Selvan, L.D., Patil, A.H., Nanjappa, V., Radhakrishnan, A., Prasad, S., Subbannayya, T., Raju, R., Kumar, M., Sreenivasamurthy, S.K., Marimuthu, A., Sathe, G.J., Chavan, S., Datta, K.K., Subbannayya, Y., Sahu, A., Yelamanchi, S.D., Jayaram, S., Rajagopalan, P., Sharma, J., Murthy, K.R., Syed, N., Goel, R., Khan, A.A., Ahmad, S., Dey, G., Mudgal, K., Chatterjee, A., Huang, T.C., Zhong, J., Wu, X., Shaw, P.G., Freed, D., Zahari, M.S., Mukherjee, K.K., Shankar, S., Mahadevan, A., Lam, H., Mitchell, C.J., Shankar, S.K., Satishchandra, P., Schroeder, J.T., Sirdeshmukh, R., Maitra, A., Leach, S.D., Drake, C.G., Halushka, M.K., Prasad, T.S., Hruban, R.H., Kerr, C.L., Bader, G.D., Iacobuzio-Donahue, C.A., Gowda, H., Pandey, A., 2014. A draft map of the human proteome. Nature 7502, 575–581.

Lansbergen, G., Komarova, Y., Modesti, M., Wyman, C., Hoogenraad, C.C., Goodson, H.V., Lemaitre, R.P., Drechsel, D.N., van Munster, E., Gadella Jr., T.W., Grosveld, F., Galjart, N., Borisy, G.G., Akhmanova, A., 2004. Conformational changes in CLIP-170 regulate its binding to microtubules and dynactin localization. J. Cell Biol. 166 (7), 1003–1014, 27.

Lee, W.-L., Oberle, J.R., Cooper, J.A., 2003. The role of the lissencephaly protein Pac1 during nuclear migration in budding yeast. J. Cell Biol. 160, 355–364.

Lenz, H., Schuchardt, I., Straube, A., Steinberg, G.A., 2006. Dynein loading zone for retrograde endosome motility at microtubule plus-ends. EMBO J. 25 (11), 2275–2286.

Liu, B., Xiang, X., Lee, Y.R., 2003. The requirement of the LC8 dynein light chain for nuclear migration and septum positioning is temperature dependent in *Aspergillus nidulans*. Mol. Microbiol. 47 (2), 291–301.

Margolin, B.S., Freitag, M., Selker, E.U., 1997. Improved plasmids for gene targeting at the his-3 locus of *Neurospora crassa* by electroporation. Fungal Genet. Newslett. 44, 34–36.

Mateja, A., Cierpicki, T., Paduch, M., Derewenda, Z.S., Otlewski, J., 2006. The dimerization mechanism of LIS1 and its implication for proteins containing the LisH motif. J. Mol. Biol. 357 (2), 621–631.

McKenney, R.J., Vershinin, M., Kunwar, A., Vallee, R.B., Gross, S.P., 2010. LIS1 and NudE induce a persistent dynein force-producing state. Cell 141 (2), 304–314.

Mesngon, M.T., Tarricone, C., Hebbar, S., Guillotte, A.M., Schmitt, E.W., Lanier, L., Musacchio, A., King, S.J., Smith, D.S., 2006. Regulation of cytoplasmic dynein ATPase by Lis1. J. Neurosci. 26 (7), 2132–2139.

Miller, J.Q., 1963. Lissencephaly in 2 siblings. Neurology 13, 841–850.

Mimori-Kiyosue, Y., Shiina, N., Tsukita, S., 2000a. The dynamic behavior of the APC-binding protein EB1 on the distal ends of microtubules. Curr. Biol. 10, 865–868.

Mimori-Kiyosue, Y., Shiina, N., Tsukita, S., 2000b. Adenomatous polyposis coli (APC) protein moves along microtubules and concentrates at their growing ends in epithelial cells. J. Cell Biol. 148, 505–518.

Minke, P.F., Lee, I.H., Tinsley, J.H., Bruno, K.S., Plamann, M., 1999. *Neurospora crassa* ro-10 and ro-11 genes encode novel proteins required for nuclear distribution. Mol. Microbiol. 32, 1065–1076.

Morris, N.R., Efimov, V.P., Xiang, X., 1998. Nuclear migration, nucleokinesis and lissencephaly. Trends Cell Biol. 8 (12), 467–470.

Morris, N.R., Xiang, X., Beckwith, S.M., 1995. Nuclear migration advances in fungi. Trends Cell Biol. 5 (7), 278–282.

Mouriño-Pérez, R.R., Linacre-Rojas, L.P., Román-Gavilanes, A.I., Lew, T.K., Callejas-Negrete, O.A., Roberson, R.W., Freitag, M., 2013. MTB-3, a microtubule plus-end tracking protein (+TIP) of *Neurospora crassa*. PLoS One 8 (8), e70655. http://dx.doi.org/10.1371/journal.pone.0070655, 12.

Mouriño-Pérez, R.R., Roberson, R.W., Bartnicki-García, S., 2006. Microtubule dynamics and organization during hyphal branching in *Neurospora crassa*. Fungal Genet. Biol. 43, 389–400. http://dx.doi.org/10.1016/j.fgb.2005.10.007.

Nédélec, F.T., Surrey, T., Karsenti, E., 2003. Self-organization and forces in the microtubule cytoskeleton. Curr. Opin. Cell Biol. 15 (7), 118–124.

Ninomiya, Y., Suzuki, K., Ishii, C., Inoue, H., 2004. Highly efficient gene replacements in *Neurospora* strains deficient for non homologous end-joining. Proc. Natl. Acad. Sci. USA 101, 12248–12253.

Oakley, B.R., 2000. An abundance of tubulins. Trends Cell Biol. 10 (12), 537–542.

Oakley, B.R., Morris, N.R., 1980. Nuclear movement is β-tubulin-dependent in *Aspergillus nidulans*. Cell 19 (1), 255–262.

Osmani, A.H., Osmani, S.A., Morris, N.R., 1990. The molecular cloning and identification of a gene product specifically required for nuclear movement in *Aspergillus nidulans*. J. Cell Biol. 111 (2), 543–551.

Perez, F., Diamantopoulos, G.S., Stalder, R., Kreis, T.E., 1999. CLIP-170 highlights growing microtubule ends *in vivo*. Cell 96, 517–527.

Plamann, M., Minke, P.F., Tinsley, J.H., Bruno, K., 1994. Cytoplasmic dynein and centractin are required for normal nuclear distribution in filamentous fungi. J. Cell Biol. 127, 139–149.

Ramos-García, S.L., Roberson, R.W., Freitag, M., Bartnicki-García, S., Mouriño-Pérez, R.R., 2009. Cytoplasmic bulk flow propels nuclei in mature hyphae of *Neurospora crassa*. Eukaryot. Cell 8 (12), 1880–1890.

Reiner, O., Albrecht, U., Gordon, M., Chianese, K.A., Wong, C., Gal-Gerber, O., Sapir, T., Siracusa, L.D., Buchberg, A.M., Caskey, C.T., et al., 1995. Lissencephaly gene (LIS1) expression in the CNS suggests a role in neuronal migration. J. Neurosci. 15, 3730–3738.

Rickard, J.E., Kreis, T.E., 1991. Binding of pp170 to microtubule is regulated by phosphorylation. J. Biol. Chem. 266, 17597–17605.

Riquelme, M., Roberson, R.W., McDaniel, D.P., Bartnicki-García, S., 2002. The effects of ropy-1 mutation on cytoplasmic organization and intracellular motility in mature hyphae of *Neurospora crassa*. Fungal Genet. Biol. 37 (2), 171–179.

Sambrook, J., Fritsch, E.F., Maniatis, T., 1989. Molecular Cloning: A Laboratory Manual Cold Spring Harbor Laboratory Press, Cold Spring Harbor, NY.

Sapir, T., Elbaum, M., Reiner, O., 1997. Reduction of microtubule catastrophe events by LIS1, platelet-activating factor acetylhydrolase subunit. EMBO J. 16, 6977–6984.

Seiler, S., Plamann, M., Schliwa, M., 1999. Kinesin and dynein mutants provide novel insights into the roles of vesicle traffic during cell morphogenesis in *Neurospora*. Curr. Biol. 9, 779–785.

Sheeman, B., Carvalho, P., Sagot, I., Geisser, J., Kho, D., Hoyt, M.A., Pellman, D., 2003. Determinants of *S. cerevisiae* dynein localization and activation: implications for the mechanism of spindle positioning. Curr. Biol. 13, 364–372.

Smith, D.S., Niethammer, M., Ayala, R., Zhou, Y., Gambello, M.J., Wynshaw-Boris, A., Tsai, L.H., 2000. Regulation of cytoplasmic dynein behavior and microtubule organization by mammalian Lis1. Nat. Cell Biol. 2, 767–775.

Steinberg, G., Wedlich-Söldner, R., Brill, M., Schulz, I., 2001. Microtubules in the fungal pathogen *Ustilago maydis* are highly dynamic and determine cell polarity. J. Cell Sci. 114, 609–622.

Straube, A., Brill, M., Oakley, B.R., Horio, T., Steinberg, G., 2003. Microtubule organization requires cell cycle-dependent nucleation at dispersed cytoplasmic sites: polar and perinuclear microtubule organizing centers in the plant pathogen *Ustilago maydis*. Mol. Biol. Cell 14, 642–657.

Straube, A., Enard, W., Berner, A., Wedlich-Söldner, R., Kahmann, R., Steinberg, G., 2001. A split motor domain in a cytoplasmic dynein. EMBO J. 20, 5091–5100.

Tarricone, C., Perrina, F., Monzani, S., Massimiliano, L., Kim, M.H., Derewenda, Z.S., Knapp, S., Tsai, L.H., Musacchio, A., 2004. Coupling PAF signaling to dynein regulation: structure of LIS1 in complex with PAF-acetylhydrolase. Neuron 44 (5), 809–821.

Tinsley, J.H., Minke, P.F., Bruno, K.S., Plamann, M., 1996. P150Glued, the largest subunit of the dynactin complex, is nonessential in *Neurospora* but required for nuclear distribution. Mol. Biol. Cell 7, 731–742.

Uchida, M., Mouriño-Pérez, R.R., Freitag, M., Bartnicki-Garcia, S., Roberson, R.W., 2008. Microtubule dynamics and the role of molecular motors in *Neurospora crassa*. Fungal Genet. Biol. 45, 683–692.

Valetti, C., Wetzel, D.M., Schrader, M., Hasbani, M.J., Gill, S.R., Kreis, T.E., Schroer, T.A., 1999. Role of dynactin in endocytic traffic: effects of dynamitin overexpression and colocalization with CLIP-170. Mol. Biol. Cell 10, 4107–4120.

Valinluck, M., Ahlgren, S., Sawada, M., Locken, K., Banuett, F., 2010. Role of the nuclear migration protein Lis1 in cell morphogenesis in *Ustilago maydis*. Mycologia 102 (3), 493–512.

Vallee, R.B., Tsai, J.W., 2006. The cellular roles of the lissencephaly gene LIS1, and what they tell us about brain development. Genes Dev. 20 (11), 1384–1393.

Vaughan, K.T., Tynan, S.H., Faulkner, N.E., Echeverri, C.J., Vallee, R.B., 1999. Colocalization of cytoplasmic dynein with dynactin and CLIP-170 at microtubule distal ends. J. Cell Sci. 112, 1437–1447.

Vaughan, P.S., Miura, P., Henderson, M., Byme, B., Vaughan, K.T., 2002. A role for regulated binding of $p150^{glued}$ to microtubule plus ends in organelle transport. J. Cell Biol. 158, 305–319.

Verdín, J., Bartnicki-Garcia, S., Riquelme, M., 2009. Functional stratification of the Spitzenkörper of *Neurospora crassa*. Mol. Microbiol. 74 (5), 1044–1053.

Xiang, X., Osmani, A.H., Osmani, S.A., Xin, M., Morris, N.R., 1995. NudF, a nuclear migration gene in *Aspergillus nidulans*, is similar to the human LIS-1 gene required for neuronal migration. Mol. Biol. Cell 6, 287–310.

Xiang, X., Plamann, M., 2003. Cytoskeleton and motor proteins in filamentous fungi. Curr. Opin. Microbiol. 6 (6), 628–633.

Yamada, M., Toba, S., Yoshida, Y., Haratani, K., Mori, D., Yano, Y., Mimori-Kiyosue, Y., Nakamura, T., Itoh, K., Fushiki, S., Setou, M., Wynshaw-Boris, A., Torisawa, T., Toyoshima, Y.Y., Hirotsune, S., 2008. LIS1 and NDEL1 coordinate the plus-end-directed transport of cytoplasmic dynein. EMBO J. 27 (19), 2471–2483.

Yao, X., Zhang, J., Zhou, H., Wang, E., Xiang, X., 2012. In vivo roles of the basic domain of dynactin p150 in microtubule plus-end tracking and dynein function. Traffic 13 (3), 375–387.

Zhang, J., Li, S., Fischer, R., Xiang, X., 2003. Accumulation of cytoplasmic dynein and dynactin at microtubule plus ends in *Aspergillus nidulans* is kinesin dependent. Mol. Biol. Cell 14 (4), 1479–1488.

Zhang, J., Zhuang, L., Lee, Y., Abenza, J.F., Peñalva, M.A., Xiang, X., 2010. The microtubule plus-end localization of *Aspergillus* dynein is important for dynein-early-endosome interaction but not for dynein ATPase activation. J. Cell Sci. 123, 3596–3604.